Nanostructured materials for thermoelectric applications

Sabah K. Bux,†[ab] Jean-Pierre Fleurial*[b] and Richard B. Kaner*[a]

Received 17th July 2010, Accepted 1st September 2010
DOI: 10.1039/c0cc02627a

Recent studies indicate that nanostructuring can be an effective method for increasing the dimensionless thermoelectric figure of merit (ZT) in materials. Most of the enhancement in ZT can be attributed to large reductions in the lattice thermal conductivity due to increased phonon scattering at interfaces. Although significant gains have been reported, much higher ZTs in practical, cost-effective and environmentally benign materials are needed in order for thermoelectrics to become effective for large-scale, wide-spread power and thermal management applications. This review discusses the various synthetic techniques that can be used in the production of bulk scale nanostructured materials. The advantages and disadvantages of each synthetic method are evaluated along with guidelines and goals presented for an ideal thermoelectric material. With proper optimization, some of these techniques hold promise for producing high efficiency devices.

Introduction

Recently there has been a surge of interest in reducing the demand for fossil fuels by developing alternative renewable energy technologies. As a result, research has been rekindled in the field of thermoelectrics. Thermoelectric devices are a promising method for alleviating some of the demand for fossil fuels in power generation and cooling. Although far from a total solution to the global energy problem, with increasing efficiency, lower costs of production, and the use of abundant and environmentally benign materials, thermoelectric devices could soon play a more significant role in our daily lives.[1]

Devices based upon the thermoelectric effect can be used for a variety of applications from power generation for deep space science exploration probes,[2] waste heat recovery in automobiles[3] and in energy intensive industrial processes[4] to electronic cooling and heating.[5] These solid-state devices are governed by one of two phenomena, the Seebeck effect, which can be used for power generation, and the Peltier effect for electronic cooling or heating. A thermoelectric device is formed when an n-type doped material is connected electrically in series and thermally in parallel across a temperature differential to a p-type doped material so that current flows between the

[a] *Department of Chemistry and Biochemistry and California NanoSystems Institute, University of California Los Angeles, 607 Charles E. Young Drive Box 951569, Los Angeles, California, 90095, USA. E-mail: kaner@chem.ucla.edu; Fax: +1 310-825-5490; Tel: +1 310-825-5346*
[b] *†Power and Sensor Systems, Thermal Energy Conversion Technologies, Jet Propulsion Laboratory/California Institute of Technology, 4800 Oak Grove Drive, MS 277-207, Pasadena, California, 91109, USA. E-mail: jean-pierre.fleurial@jpl.nasa.gov; Tel: +1 818-354-4144*
† Current address

Sabah K. Bux

Sabah K. Bux received her Bachelors of Science in Chemistry, Magna Cum Laude from California State Polytechnic University Pomona in 2005. She joined UCLA in 2005 as a graduate student working with Professor Richard Kaner on nanostructured materials for thermoelectric applications and received her PhD in inorganic chemistry in 2010. She has earned UCLA Edwin Pauley, NSF-IGERT, NASA-GSRP fellowships and is a NASA student ambassador. Currently she is an engineer at the Jet Propulsion Laboratory working with Dr Jean-Pierre Fleurial, where she continues her work on thermoelectrics.

Jean-Pierre Fleurial

Jean-Pierre Fleurial is the group supervisor of the Thermal Energy Conversion Technologies group at JPL. Dr Fleurial earned his PhD in solid state physics and materials science from the National Polytechnique Institute of Lorraine, France, in 1988. In 1988, Dr Fleurial came to JPL as a National Research Council Resident Research Associate and joined the permanent staff in 1990. He was first involved with the optimization of Si–Ge alloys for thermoelectric power generation. More recently, Dr Fleurial has been actively involved with the study of novel thermoelectric materials, in particular compound nanostructured materials. Dr Fleurial has served on the board of the International Thermoelectric Society.

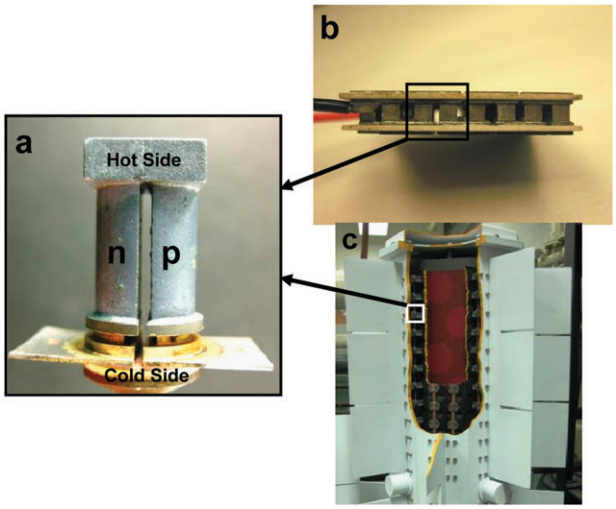

Fig. 1 Thermoelectric devices consist of: (a) single n-type and p-type conductivity materials connected together to form a couple; (b) a series of couples forms a thermoelectric module that can be used for small scale electronic heating or cooling applications and (c) an array of thermoelectric modules coupled to heat exchangers constitutes a thermoelectric generator.

two materials. The device can harvest a heat source and do work once connected to an external resistive load or conversely, heat can be pumped across a temperature differential if connected to an electrical power source. Fig. 1 shows a progression of a thermoelectric device starting with a pair of n- and p-type materials known as a thermoelectric couple (Fig. 1a). When several couples are connected together electrically in series and thermally in parallel, this is known as a thermoelectric module (Fig. 1b). Several modules interfaced with heat exchangers coupled to a heat source and heat sink constitute a thermoelectric generator (Fig. 1c).

1 Thermoelectric effect

If a temperature gradient is applied along a conducting sample, the charge carriers which were initially uniformly distributed are perturbed and the free carriers (either electrons for an n-type material or holes for a p-type material) diffuse from the hot end to the cold end, resulting in an electromotive force (emf) (Fig. 2a). When the material is subjected to a temperature gradient (ΔT), the open circuit voltage (V_{oc}) with no current flowing is known as the Seebeck voltage, which is given by $V_{oc} = S(\Delta T)$, where S is the Seebeck coefficient in units of $\mu V\ K^{-1}$.[6]

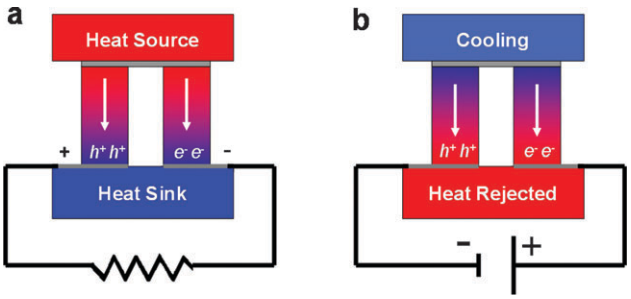

Fig. 2 Thermoelectrics: (a) the Seebeck effect: if a temperature gradient is applied along a conducting sample, the charge carriers are disturbed and the free carriers (either electrons for an n-type material or holes for a p-type material) diffuse from the hot end to the cold end, resulting in a back emf. Once connected to an external load, the device can do work and thermal energy can be harvested. (b) The Peltier effect: conversely, when an electrical current is applied a temperature gradient is generated. The direction of heat pumping depends on the direction of the electrical current.

Conversely, the Peltier effect is observed when an electrical current (I) is applied to a conducting material, generating a temperature gradient. Depending on the direction of the current, I, each side can become either hot or cold (Fig. 2b). The rate of reversible heat absorption, $\dot{Q}$, is given by $\dot{Q} = \Pi I$, where Π is the Peltier coefficient and is expressed in units of V.[6]

Although thermoelectric effects have been known for over 200 years,[7,8] relatively low conversion efficiencies have limited these devices to niche applications with unique reliability and scalability requirements such as space power applications and small-scale refrigeration. For the past 50 years, the National Aeronautics and Space Administration (NASA) has utilized thermoelectrics in their space science and exploration missions. Thermoelectrics are generally used in deep space missions where the solar flux is too low for photovoltaics to be effective (typically beyond 5 a.u.) or for extended missions on the surface of Mars or the Moon, where the day/night cycle, settling of dust, sun exposure and lifetime requirements limit the usefulness of photovoltaics. Thermoelectric generators have been demonstrated to be extremely reliable, durable and long-lived power sources.[9] In order to expand into larger scale power generation applications such as waste heat recovery from automobiles[3] or industrial processing plants,[4] significantly higher materials thermal-to-electric conversion efficiency and lower costs of production for thermoelectric materials and systems are necessary. Additionally, for large-scale terrestrial applications, such as waste heat recovery, the ability to achieve these metrics with environmentally benign materials is highly desirable.

Richard B. Kaner

Richard B. Kaner is a Professor of Chemistry and a Professor of Materials Science and Engineering at UCLA. He received a PhD in inorganic chemistry from the University of Pennsylvania in 1984, followed by postdoctoral research at the University of California, Berkeley. He joined the University of California, Los Angeles (UCLA) in 1987 as an Assistant Professor, earned tenure in 1991 and became a Full Professor in 1993. Professor Kaner has received awards from the Dreyfus, Fulbright, Guggenheim and Sloan Foundations as well as the Exxon Fellowship in Solid State Chemistry, the Buck-Whitney Research Award and the Tolman Medal from the American Chemical Society.

The thermoelectric conversion efficiency, η, of a material is defined as the product of the Carnot efficiency and a materials conversion efficiency factor, f, which is directly related to the dimensionless thermoelectric figure of merit (ZT) as given in eqn (1):

$$\eta = \frac{\Delta T}{T_h} f(\mathrm{ZT}) \quad (1)$$

where f is defined as (eqn (2)):

$$f = \frac{\sqrt{1+\mathrm{ZT}}-1}{\sqrt{1+\mathrm{ZT}}+\frac{T_c}{T_h}} \quad (2)$$

The thermoelectric figure of merit (ZT) is defined in eqn (3) as:

$$\mathrm{ZT} = \frac{S^2}{\rho\lambda} T \quad (3)$$

where S is the Seebeck coefficient, ρ is the electrical resistivity, T is the absolute temperature and λ is the total thermal conductivity which is the sum of both an electronic contribution (λ_e) and a lattice contribution(λ_L). In order to achieve high ZT values, materials must possess a unique combination of electrical and thermal transport properties: a low metal-like electrical resistivity, a high insulator-like Seebeck coefficient, and a low glass-like thermal conductivity. Typically, the best thermoelectric materials with the optimum Seebeck coefficient and electrical conductivity are heavily doped semiconductors with 10^{19} to 10^{20} charge carriers per cubic centimetre,[10] as described in Fig. 3a.

In addition to having favorable electrical transport properties, a good thermoelectric material must also have low thermal conductivity. The lattice thermal conductivity (λ_L) is the result of movement by heat carrying phonons through the lattice while the electronic thermal conductivity (λ_e) is the heat contribution from the charge carriers (electrons or holes) moving through the lattice. For extrinsically doped materials with negligible mixed conduction effects, the electronic thermal conductivity can be calculated from the Widemann–Franz law: $\lambda_e = L\sigma T$. The constant, L, is known as the Lorenz factor and it relates to the coupling between charge carriers and phonons in a given class of materials. Therefore, a material with a relatively high electrical conductivity will also have a relatively high total thermal conductivity. This interdependency of thermal and electronic terms is a limiting factor in the search for materials with a high ZT, *i.e.* any improvement in the electrical transport terms often has a deleterious effect on the thermal transport terms and *vice versa*. In spite of extensive experimental and theoretical research, the peak ZT value has long been limited to about 1.2 for both p-type and n-type materials across the temperature range from 100 K to 1500 K.[11] New theoretical insights indicate that substantial gains can be achieved with new materials, structures and chemistries, while novel material synthetic techniques offer improved experimental control that could enable effective testing of these ideas.

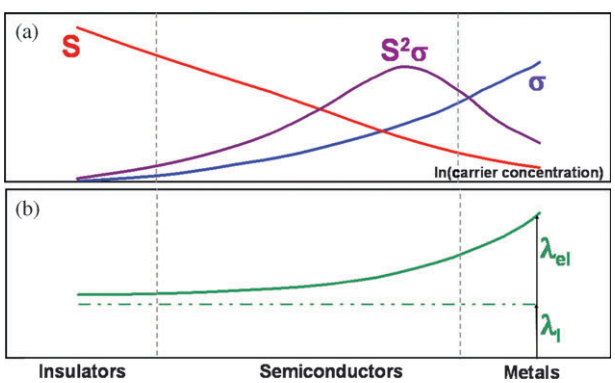

Fig. 3 (a) The interdependency of (a) the Seebeck coefficient (S), electrical conductivity (σ) and (b) the lattice (λ_l) and electronic (λ_e) contributions to the thermal conductivity for insulators, semiconductors and metals.

1.1 A brief recent history of thermoelectrics. Historically, the leading method in order to improve the ZT of thermoelectric materials was to optimize good bulk thermoelectric materials, such as Bi_2Te_3, PbTe and $Si_{1-x}Ge_x$, that were identified in the 1950s.[9] In the 1960s, the leading method for increasing ZT was to control doping and form solid-solutions such as Bi_2Te_3–Sb_2Te_3,[12] PbTe–SnTe,[13] and $Si_{1-x}Ge_x$.[14] This was an effective way of reducing the lattice thermal conductivity *via* point defect scattering of phonons. Point defect scattering serves to decrease the lattice thermal conductivity by increasing the frequency and magnitude of the scattering events for the heat carrying phonons. Although significant reductions in the lattice thermal conductivity were achieved, there were also concurrent reductions in the charge carrier mobility, thus limiting the overall ZT enhancement.

1.2 Methods for improving ZT. Decoupling the thermal and electronic terms has been a key strategy in order to improve ZT. In the 1980s and 1990s "self-assembling" and "force-engineering" approaches were used. In the "self-assembly" approach, layered chalcogenide materials were synthesized from a melt using Bi_2Te_3, GeTe and PbTe building blocks.[15] In the "force-engineered" approach, the idea was to use powder metallurgical techniques and either reduce grain size to a few microns[16] or add nanoscale inert scattering centers.[17] Another "force-engineered" approach was to introduce defects *via* neutron radiation.[18] Although the ZT improvements using these techniques were marginal, they did give valuable insights into the thermal and electrical transport mechanisms.

In the search for materials with a high thermoelectric figure of merit, there emerged two leading concepts: either the examination of complex crystal structures with low lattice thermal conductivities or the investigation of low-dimensional structures allowing for atomic level control of nanoscale features. The movement to examine complex materials first came from the idea that an ideal thermoelectric material should combine the low thermal conductivity of a glass with the electronic properties of a single crystal. This "phonon glass electron crystal" (PGEC) approach, coined by Glen Slack in the mid 1990s, was theorized to be the most achievable in materials with a complex symmetry and crystal structure, where the presence of voids (vacancies) and rattlers (atoms with large atomic displacement parameters located in "cages" of some of these structures) would act as highly effective

phonon scattering sites and dramatically reduce the lattice thermal conductivity.[21] Although the perfect PGEC material has yet to be synthesized, the idea spurred a significant amount of research in complex materials systems[11] such as Skutterudites,[22,23] Zintl phases,[24] and Clathrates[25,26] for which high peak ZT values (1.0 to 1.5) were obtained.

In the early 1990s Hicks and Dresselhaus theorized that low-dimensional materials could have significant increases in ZT.[27] The ZT enhancement would be a result of an improved Seebeck coefficient from an increased density of states by quantum confined charge carriers.[27] Soon after the publication of this theory, it was reported that thin film structures based on Bi_2Te_3–Sb_2Te_3 superlattices[28] and PbTe–PbSe quantum dot structures[29] initially demonstrated significant increases in ZT. The large ZT enhancements were not due to the improvement in the Seebeck coefficient, but were instead attributed to a large decrease in the lattice thermal conductivity brought about by interfacial scattering of phonons, thus spurring a significant amount of research in the field of low-dimensional thermoelectric materials. This approach has been expanded to include nanowires[30,31] and GaAs/AlAs/ErAs[32,33] and Si/SiGe superlattices.[34–36] Excellent reviews on these low-dimensional systems can be found in ref. 37–40. It should be noted that the earlier work on PbTe–PbS quantum dot structures was recently re-investigated. Originally, the thermal conductivity of these thin film structures was measured indirectly. A recent re-measurement of the thermal conductivity using a diffuse reflectance thermal conductivity technique indicates that the lattice thermal conductivity was not as low as initially thought and therefore the ZT was much lower than what was originally reported.[41] In any case, preliminary results on the low-dimensional materials spawned a new wave of research into nanoscale materials that do have low lattice thermal conductivities.

Although these low-dimensional structures have demonstrated high preliminary ZTs, they are ill-suited for high temperature applications that require long-term thermal and mechanical stability as well as effective, practical coupling to existing heat sources and heat sinks. Additionally, scale-up to kilogram quantities could also be very challenging in order to fabricate the required macro-sized devices.

A relatively new strategy is to learn from the promising results achieved for low-dimensional materials and design novel bulk materials with low lattice thermal conductivities and good electrical properties.[42] There have been promising initial results that indicate that large ZT enhancements can be achieved by increasing the density of interfaces through reduction of the crystal size to a few nanometres.[43] Here we focus on synthetic techniques that can be used to synthesize large quantities of nanostructured materials with desirable properties. Specifically we will examine bulk materials that have very favorable electronic properties such as Bi_2Te_3,[44] PbTe,[45] $CoSb_3$[22,46] and $Si_{1-x}Ge_x$,[47] but with relatively high bulk thermal conductivities, as seen in Fig. 4. These materials could benefit most from a nanostructuring approach that minimizes the lattice thermal conductivity. Additionally, we provide a general set of requirements for an ideal nanostructured bulk synthetic technique enabling the creation of materials for practical devices.

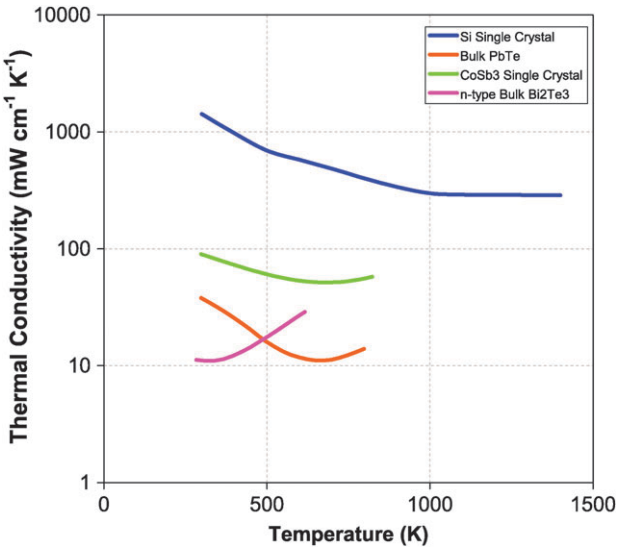

Fig. 4 Bulk thermal conductivities of heavily doped Bi_2Te_3[19] (pink), PbTe[19] (orange), $CoSb_3$[19] (green) and Si[20] (blue). These materials possess excellent electrical transport properties; however, they also have very high thermal conductivities.

2. Nanostructured bulk thermoelectrics

The concept of reducing the grain size to reduce thermal conductivity and enhance ZT has been known for some time. Rowe *et al*. in the 1980s demonstrated a reduction in the lattice thermal conductivity by about 20% for $Si_{0.80}Ge_{0.20}$ by reducing the grain size to a few microns.[16] In the 1990s, Mahan suggested that nanostructuring on the bulk scale would be an ideal method of enhancing ZT for practical devices.[48] But only recently has this concept become experimentally feasible and the resulting materials characterizable using high resolution imaging techniques. The "nanostructured bulk" concept is relatively simple: reduce the lattice thermal conductivity in a thermoelectric material by increasing phonon scattering over a large mean-free path range while maintaining good electrical properties. Theoretically, nanostructuring serves to introduce a large density of interfaces in which phonon scattering can occur without having to compromise carrier mobility values, due to the much shorter mean-free path of electrons *vs.* phonons in heavily doped semiconductors. As an example, theoretical modeling on the contribution of phonon scattering to the lattice thermal conductivity as a function of the mean-free path for Si was conducted. The calculations indicated that 90% of the thermal conductivity accumulation in Si is due to phonons that have a mean-free path greater than 20 nm.[49] Therefore, if the grain size were reduced to 20 nm, a 90% reduction in the lattice thermal conductivity could be achieved. The carrier mobility should not be affected as the electron mean-free path in Si was calculated to be only a few nanometres.[20] The guidelines for the nanoparticle dimensions vary for different material systems, but the critical feature sizes necessarily remain in the nanoscale (5 to 50 nm). It is anticipated that in order to fully optimize the thermoelectric properties of a material will require composite structures with controlled distributions of nanoscale particles discrete in size and possibly in composition.

Experimentally achieving good control at the nanoscale level in practical bulk materials clearly constitutes a very significant challenge for years to come, and various synthetic methods in order to produce bulk scale quantities of thermoelectric materials are evaluated in the next section.

2.1 Guidelines for the synthesis of effective nanostructured materials. The goal is to successfully decouple the thermal and electronic transport terms and, in theory, nanostructured materials are predicted to be an effective method for achieving this. The difficulty lies in trying to find the best synthetic/fabrication method that can produce large quantities of materials that meet the rigor that is required for a bulk device, in particular, thermal stability and mechanical integrity. Additionally, in order to expand into large-scale applications such as waste heat recovery, the material conversion efficiency and operating temperature range, material abundance, cost of production and toxicity all need to be considered. Ideally, there are four considerations that should serve as a guide in developing synthetic approaches to nanoscale bulk materials for practical applications: (1) the synthetic technique needs to be scalable and relatively low-cost, since practical applications eventually require kilograms of materials. The technique should also provide good control over particle size, distribution and morphology; (2) practical device designs require that the materials must be 95% or greater of the theoretical density depending on the material for machining/device integration and operational purposes; (3) the nanostructured bulk material should exhibit a significant enhancement in ZT over the bulk or state-of-the-art material and finally; (4) the compacted nanostructured material should be thermally stable at the planned temperatures of operation. Thermal stability is a key aspect, since in practical power generation applications thermoelectric devices must operate for extended periods of time under steady-state or thermal cycling conditions. There is no gain in synthesizing nanostructured materials if the nanoscale features are lost through grain growth or diffusion after being heated for an extended period of time.

3. Methods for synthesizing bulk quantities of nanostructured materials

There exist several methods for producing nanoscale materials: electrochemical synthesis,[31,50–52] chemical vapor deposition,[53] molecular beam epitaxy,[29,30] pulsed laser ablation[53] and pyrolysis of volatile precursors.[54–56] Although, these methods have been demonstrated to produce beautiful nanostructured materials of various geometries and complexities, they have inherent limitations that often include complex and expensive equipment, toxic precursors and scale-up challenges. Alternative methods for synthesizing large scale quantities of nanostructured materials include solvothermal/hydrothermal methods, solution-based synthesis, self-assembly/nanoprecipitation techniques, and high energy ball milling. The advantages and disadvantages of each of these techniques will be discussed in relation to the criteria for an ideal nanoscale thermoelectric material.

3.1 Solvothermal/hydrothermal synthesis of nanoscale thermoelectric materials. The solvothermal or hydrothermal technique has been proposed as a possible method for synthesizing large quantities of nanostructured materials. This method has been used effectively for several years to grow semiconductor materials of various geometries from large ingots to nanostructured materials.[61] Recently it has been applied to nanostructured thermoelectric materials.[62] The solvothermal or hydrothermal method has been used to produce nanostructured Bi_2Te_3,[58,60,61,63] PbTe[57] and $CoSb_3$[59,64–66] with varying morphologies and particle size distributions (Fig. 5). In this method, precursor materials (usually metal oxides or halides) in the specific end-product stoichiometry are combined with a reducing agent in the presence of either a solvent (solvothermal method) or an aqueous solution (hydrothermal method) which is then loaded into an autoclave and sealed. The mixture is then pressurized and heated to a temperature above the critical point of the solvent, where it is held for a desired period of time, and then cooled to room temperature. The nanostructured product is then extracted and isolated from the residual salts.[61]

3.1.a Advantages of the solvothermal/hydrothermal technique. A significant advantage of using the solvothermal/hydrothermal technique is that the morphology of the end-product can be controlled by simply adding a templating ligand.[61] The ligand acts as a chelating agent with the reduced ionic precursors, leading to unique coordination geometries, which yield various morphologies.[58] Common templating ligands that have been used include ethylenediaminetetraacetic acid (EDTA),[61] polyvinylpyrrolidone,[61] pyridine,[62] propane-1,3-diamine,[63] and ethylenediamine.[57] With the aid of these templating agents, various morphologies have been achieved including: PbTe nanocubes,[57] Bi_2Te_3 nano-flowers,[58] $CoSb_3$ and Bi_2Te_3 nanoparticles,[57,61] Bi_2Te_3 nanowires,[61] and Bi_2Te_3 nanosheets[67] (Fig. 5). A good review of the reaction mechanism during a solvothermal reaction can be found in ref. 61. Additionally, once the precursors are dispersed homogeneously

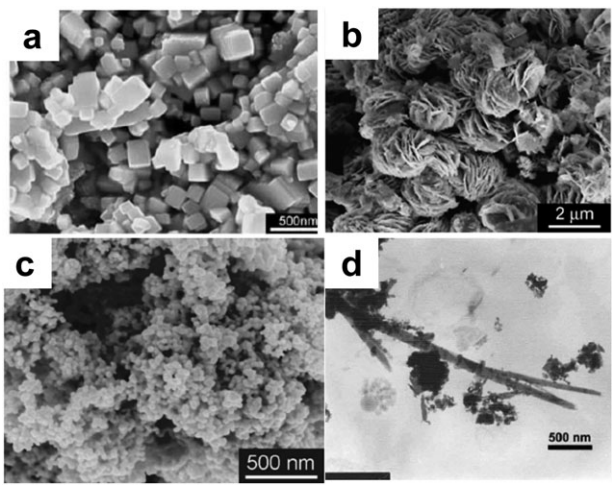

Fig. 5 Electron micrographs of products using solvothermal/hydrothermal methods. (a) PbTe nanocubes[57] [adapted from ref. 57. Copyright 2007 Springer], (b) Bi_2Te_3 nanoflowers[58] [adapted from ref. 58. Copyright 2007 Elsevier], (c) $CoSb_3$ nanoparticles[59] [adapted from ref. 59. Copyright 2007 American Institute of Physics], (d) Bi_2Te_3 nanowires[60] [adapted from ref. 60. Copyright 2004 Elsevier].

and reduced in the solvent matrix with a templating ligand, relatively uniform particle sizes can be achieved[63] ranging from 20–30 nm for Bi_2Te_3 nanoparticles[57,61,63,68] to 100 nm for PbTe nanocubes[57] (Fig. 5a), to 10–50 nm for $CoSb_3$ nanoparticles[65,66] (Fig. 5c).

The solvothermal technique can also be used as a method for coating nanoparticles or making nanoparticle composites. In the work by Tritt and co-workers, bulk-scale thermoelectric materials were coated with nanoparticles[65] or with alkali metals as a method of increasing the electronic properties *via* "grain-boundary engineering". The idea is to increase the Seebeck coefficient by grain boundary filtering of the charge carriers.[65,68]

3.1.b Disadvantages of the solvothermal/hydrothermal technique. The solvothermal/hydrothermal technique has been demonstrated to have excellent control over morphology and relatively narrow particle size distribution. There are a few disadvantages: one problem is the lack of control over stoichiometry, particularly with $CoSb_3$-based alloys, where it can be difficult to make phase pure products. Mi and coworkers attempted to synthesize p-type $CoSb_3$ *via* a solvothermal route but ended up with n-type conduction due to the presence of $CoSb_2$ impurities and non-stoichiometry.[59] Phase segregation into the more thermally stable $CoSb_2$ phase is a common problem in the synthesis of $CoSb_3$ and even occurs with bulk synthesis from the melt.[69] Similarly, this problem can be seen in the synthesis of Bi_2Te_3, where free Bi and Te were found in the product.[60]

These stoichiometric deviation problems can make it difficult to effectively control the doping level and carrier concentration, since each is very sensitive to changes by a few fractions of an atomic percent. With some fine-tuning and evaluation of the reaction kinetics, phase pure $CoSb_3$ can be obtained. This was demonstrated by Li and coworkers who showed that phase pure Fe-doped $CoSb_3$ can be synthesized by simply facilitating the interdiffusion of the Co and Sb ions by increasing the temperature in their reaction scheme.[66] Unfortunately, no thermoelectric properties were reported.

Another problem with the solvothermal/hydrothermal method is that materials can be difficult to sinter[59] leading to low densities. Zhang and co-workers reported densities for Bi_2Te_3 of only 86–91% of the theoretical density.[58]

Fourier Transform Infrared spectroscopy (FT-IR) on hydrothermal/solvothermally synthesized materials showed that after product isolation, residual oxides and organics remained. The residual oxides likely comes from either the washing/isolation of the nanoparticles or from the salts post-synthesis or from the solvents themselves. The presence of organics may be due to the solvents being adsorbed onto the surface of the nanoparticles.[63] Hence the oxide layer and residual solvent can prevent effective grain coarsening and prevent sintering, leading to low density materials, and reductions in the electrical conductivity.

3.1.c Summary of solvothermal/hydrothermal technique. Although this method can provide excellent control over morphology and particle size distribution, controlling stoichiometry and obtaining dense materials can be difficult. These issues can be problematic for practical thermoelectric applications as the lack of stoichiometry and low density can adversely affect the electrical transport properties of the materials. With proper manipulation of some kinetic parameters, the stoichiometry can be controlled. Additionally, oxide and residual solvent, in theory, could be removed if an effective post-treatment process can be developed.

3.2 Solution-based synthesis of nanostructured thermoelectric materials. Another potential method for the synthesis of large-scale quantities of thermoelectric materials is *via* solution-based or wet-chemical synthesis. A solution-based synthesis is similar to the solvothermal process in that a stoichiometric ratio of precursor materials is dissolved or dispersed in a solvent and the product is usually precipitated out either by manipulating the pH or by the addition of a reductant. Unlike the solvothermal/hydrothermal method, the entire reaction occurs under ambient pressure. This method has been used to synthesize a variety of thermoelectric materials including $CoSb_3$[64,75–78] (Fig. 6a), PbTe[79–84] (Fig. 6b), Bi_2Te_3[57,70–74] (Fig. 6c) and Si (Fig. 6d).[85] There are several different types of solution-based syntheses for thermoelectric materials that include a modified polyol process,[75] a solution precipitation method,[64,76,77] and a synthetic scheme that is analogous to the synthesis of CdS quantum dots.[70,72,73,85,86]

In the solution precipitation method, Toprak and co-workers dissolved Co and Sb precursors in water, and then added oxalic acid to form Co and Sb oxalate complexes. Upon adding NH_4OH, 150 nm to 2 micron size particles of $CoSb_3$ nanoparticles precipitated.[77] Similarly, Yang and co-workers synthesized 30 nm $CoSb_3$ nanoparticles *via* a modified polyol synthesis. A stoichiometric amount of precursors were added

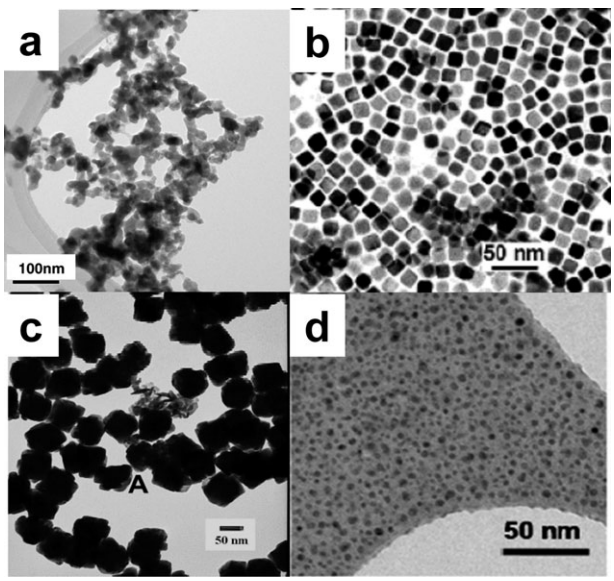

Fig. 6 Electron micrographs of products using solution based synthesis: (a) $CoSb_3$ nanoparticles[78] [adapted from ref. 78. Copyright 2009 American Institute of Physics], (b) PbTe nanocubes[80,87] [adapted from ref. 87. Copyright 2004 American Chemical Society], (c) Bi_2Te_3 nanoparticles[73] [adapted from ref. 73. Copyright 2009 American Chemical Society] and (d) Si nanoparticles[85] [adapted from ref. 85. Copyright 2006 American Chemical Society].

to a solution of polyvinylpyrrolidone and tetra-ethylene glycol. A reducing agent was added to this mixture and 30 nm $CoSb_3$ nanoparticles precipitated. The product was then isolated and washed with water.[75] In a traditional polyol process, the polyol serves as a mild reducing agent. Yang and co-workers added a stronger reducing agent, $NaBH_4$, in order to precipitate out the product.[75] The addition of a reducing agent to the solution of dissolved precursors is also an effective method for producing nanostructured materials. For example, this technique has been successfully used for the synthesis of PbTe.[57,80,82] Wan and co-workers demonstrated that by simply changing the reducing agent used, they could change the morphology of their PbTe from nanorods to nanocubes in the size range of 40–70 nm.[80]

A solution-based method that is gaining interest in the thermoelectrics community is the synthesis of quantum confined nanoparticles using methods similar to that for the synthesis of CdS quantum dots.[86] In this method, precursor solutions are separately heated, mixed, and then rapidly quenched. The resulting nanoparticles are capped with long chain alkanes or alkane thiol capping ligands to prevent agglomeration and Ostwald ripening. The capping ligands can also act as templates and be used to form different geometries.[88] Very small nanoparticles (2 nm) have been synthesized using this technique with a relatively monodisperse distribution.[85] This method is typically effective for pure compound semiconductors; recently, Zhao and Burda have demonstrated the ability to tune the Sb_2Te_3–Bi_2Te_3 alloy composition (Fig. 6c).[73]

3.2.a Advantages of solution based techniques. The advantages of the solution based method are that a very narrow particle size and distribution can be achieved. The particle size can be controlled by changing the reaction conditions such as the solvent,[75] complexing agent,[77] or by changing the capping ligand.[70] The role of the capping ligand is to coat the nanoparticles and prevent Ostwald ripening which leads to larger nanoparticles. Since, particle agglomeration is also reduced, the relative distribution of the nanoparticle sizes remains relatively narrow and with low lattice strain. Lattice strain is an issue with some of the techniques discussed later on. Another key advantage of this method is the ability to produce samples with very small particle sizes, where quantum confinement effects can be observed. This feature is difficult to attain using other synthetic methods.

3.2.b Disadvantages of solution based techniques. The main advantage of this technique is also its greatest disadvantage. In order to get the small, relatively monodisperse nanoparticles, a capping agent must be used. This capping agent can either be a surface oxide or a long chain alkane or an alkane thiol. The problem with the capping ligands is if they are not removed completely, they can cause difficultly in sintering and detrimental effects to the electrical properties.[78] It is claimed that the capping ligand can be removed by simply annealing, Dirmyer *et al.* found that upon compaction their sample had low density (only 87% of the theoretical density for PbTe) and had a relatively high concentration of n-type carriers. The increase in the carrier concentration and reduced density was attributed to the residual thiol-based ligands.[70] The effect of the incomplete removal of thiol ligands is more evident in the case of the synthesis of a $Sb_xBi_{2-x}Te_3$ solid solution *via* solution based techniques. The parent compound, $Sb_xBi_{2-x}Te_3$, is a p-type material,[44] the residual S from the thiol capping ligand changed the conduction type to strongly n-type[72] by the formation of Bi_2S_3[89] on the surface due to a reaction with the thiol ligand.

Another disadvantage of the solution based method is that it can be quite difficult to get phase pure materials, in particular for the $CoSb_3$ system. As seen with the solvothermal/hydrothermal process, the thermodynamically stable $CoSb_2$ phase forms readily[76–78] and as discussed earlier, this can make materials difficult to sinter and can negatively impact the electrical properties by disrupting the conduction type. Additionally, the residual surface oxides and organics can make the nanostructured materials difficult to sinter, thus adversely affecting both mechanical and electrical properties.

3.2.c Summary of solution based techniques. Solution-based syntheses are promising methods for producing nanostructured materials due to their ability to control particle size down to very small sizes (<5 nm), morphology, and its distribution; as discussed earlier, the capping ligands can be detrimental to the thermoelectric properties. In a study by Scheele and co-workers,[90] they have developed an interesting method of removing the capping ligands from their Bi_2Te_3 nanoparticles, which were synthesized by a similar route to that of Budra and co-workers. Under inert conditions, they carried out an exchange of the weak alkane–thiol ligands to the more favorable oleic acid capping ligands. The nanoparticles were subjected to a hydrazine hydrate/hexane mixture, in which the hydrazine served to deprotonate and remove the oleic acid and assist in oxide removal. The pure nanoparticles were then extracted in the polar hydrazine hydrate layer and the oleic acid was left in the organic hexane layer. NMR studies were carried out in order to confirm the removal of the capping ligand.[90] Although, the thermoelectric properties have yet to be optimized, the study by Scheele and co-workers presents a promising method for removing capping ligands.

It should be noted that having a surface oxide isn't always detrimental. Nolas and co-workers examined the thermoelectric properties of 100 nm PbTe nanocrystals made by a solution based technique.[81,84] They found that their samples displayed a unique carrier mobility that had not been observed in bulk PbTe. They attributed the behavior to the oxide surface, which acted as an additional charge carrier scattering center. As a result, the nanostructured materials displayed an enhanced ZT compared to bulk PbTe, suggesting that having an appropriate material at the grain boundary, or embedded in the grains as in a composite, may be a possible route to increasing ZT.[84]

3.3 Nanoprecipitation and self-assembly synthesis of nanostructured materials

3.3.a Nanoprecipitation technique. A solid-state approach to synthesizing bulk nanostructured materials is to synthesize nanostructured inclusions in bulk materials *in situ* through

nanoprecipitation. In this method, a molten material is subjected to a thermal treatment in which nanoscale inclusions are produced either by phase segregation or by spinodal decomposition. This method works well for PbTe based compounds, specifically the $AgPb_mSbTe_{2+m}$ (also known as LAST-m) family of compounds.[92] These compounds form from a solid-solution between $AgSbTe_2$ and PbTe. In order to create the nanoprecipitates, the samples were melted and then quenched and annealed at 400 °C. At this point, the materials undergo phase segregation or spinodal decomposition, thus forming nanoscale precipitates in the matrix (Fig. 7).[94] Using this technique, Kanatzidis and co-workers demonstrated that this family of LAST compounds exhibit very low thermal conductivities compared to bulk PbTe material, and as a result, ZTs up to 1.7 have been reported.[91,95] Additionally, with the addition of Ge and Sn doping, Gelbstein and co-workers report a ZT of 1.2 for $Ge_{0.50}Pb_{0.25}Sn_{0.25}Te$ using the spinodal decomposition technique.[96] Since, this method depends on a favorable phase diagram that allows for a high solubility of the component materials (*i.e.* $AgSbTe_2$ and PbTe) at temperatures which are significantly higher than the temperature needed for spinodal decomposition and nanoparticle precipitation, the operating temperature range of the nanostructured composite may be severely limited in order to maintain the nanostructured composites. This phase diagram requirement may also limit the applicability of this method to other types of chemistries.

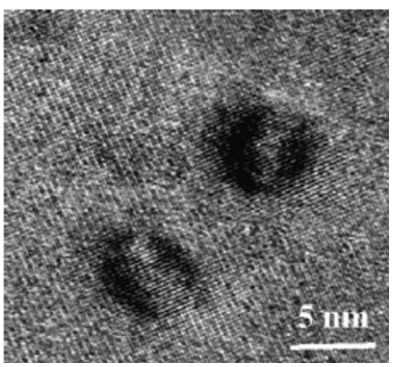

Fig. 7 A nanoscale precipitate in the LAST matrix before annealing.[91] [Adapted with permission from ref. 91. Copyright 2010 American Chemical Society.]

3.3.b Advantages and disadvantages of the nanoprecipitation technique. The main advantage of nanoprecipitation is that it is essentially an inorganic melt technique, where the nanostructured inclusions form in one step in the bulk material, with minimal processing and handling. The disadvantage of this technique is that it can be difficult to control the carrier concentration from batch to batch due to the complex nature of the materials system and the phase diagram. Additionally, accurate temperature control is a key aspect to this synthesis as even the parent $AgSbTe_2$ material is prone to phase segregation.[91,97]

3.3.c Self-assembly technique. Another related solid-state technique in which the nanostructured domains are prepared *in situ* involves the self-assembly of lamellae-like structures. The nanoscale lamellae form during the solidification or annealing steps of a mixture of two compounds. This method was first applied to thermoelectric materials by Cao *et al.*[98] who synthesized Bi_2Te_3 and Sb_2Te_3 powders using a solvothermal technique. The powders were mixed and consolidated *via* hot-pressing to 92–94% of their theoretical density. TEM imaging showed lamellae structures ranging from 5 to 50 nm.[98]

Similarly, Ikeda and co-workers examined the Sb_2Te_3 and PbTe system.[93] This system is ideal due to the $Pb_2Sb_6Te_{11}$ phase that decomposes near the eutectic of PbTe and Sb_2Te_3. Rapid cooling through this phase produces oriented lamellae of Sb_2Te_3 and PbTe with grain sizes as small as 40 nm (Fig. 8). Thermal conductivity measurements showed a reduced thermal conductivity relative to bulk PbTe.[43,101]

3.3.d Advantages and disadvantages of the self-assembly technique. The advantage is that this is a one-step technique in which the nanoscale lamellae are formed by a simple thermal treatment with minimal processing and handling. This quenching technique provides directional formation of nanoscale features which do not form by the precipitation technique discussed in the previous section. In addition, this near equilibrium process can provide very "clean", low strain interfaces favorable to electronic transport.

A disadvantage of most of the work reported to date is that it was accomplished with the PbTe–Sb_2Te_3 system. Electronically, PbTe is an n-type thermoelectric material and Sb_2Te_3 is a p-type thermoelectric material, and so mixed

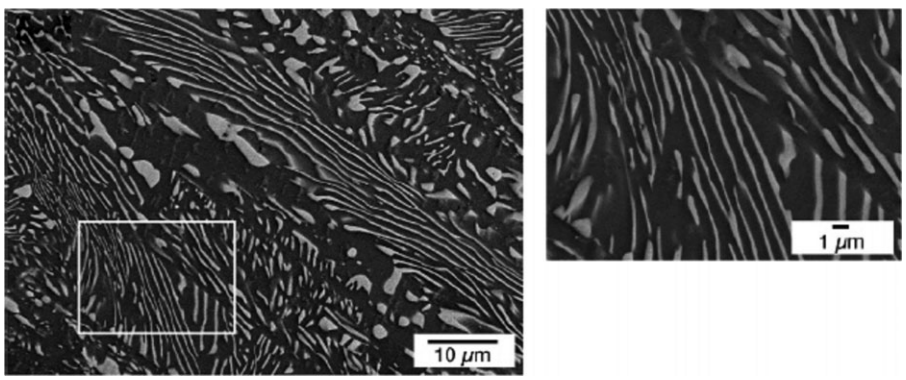

Fig. 8 Sb_2Te_3–PbTe nanoscale lamellae structures.[93] [Adapted with permission from ref. 93. Copyright 2007 American Chemical Society.]

conduction effects are very detrimental to the thermoelectric properties of bulk materials. Other chalcogenide systems that do not suffer from this shortcoming are now being explored.[102] This is a promising method of making nanostructured composite materials *in situ*.

3.4 High energy ball milling of nanostructured materials. Recently, the technique of high energy ball milling (or mechanical alloying) has attracted much attention in the synthesis of nanostructured thermoelectric materials.[20,42,103–109] This technique was initially used to synthesize Ni–Al superalloys and intermetallic compounds in the 1970s.[110]

Later on, it was found to be an effective synthetic method for making thermoelectric materials,[111,112] in particular alloys with unfavorable phase diagrams such as Si–Ge.[113] In this technique, elemental powders or intermetallic compounds are inserted into a milling vial with some ball bearings. The vial is then loaded into a high energy ball mill. The constant agitation of the ball mill causes the powders to be subjected to a series of impact collisions between the powder and ball bearings (Fig. 9).[99,100] As a result, the powders are constantly cold-welded and fractured, leading to the formation of nanostructured domains (Fig. 10). Details on the ball milling process, different types of mills, kinetics, thermodynamics and related information can be found in ref. 99.

Earlier work on the ball milling of $Si_{1-x}Ge_x$ compounds yielded micron sized grains with an overall enhancement of about 20% in ZT.[16] With modifications to the ball milling kinetics with respect to the powder to ball ratio and time, nanostructured materials were produced and the ZT increases were much more substantial, up to 250% for both n- and p-type $Si_{1-x}Ge_x$ alloys (Fig. 11).[114]

3.4.a Advantages of the ball milling technique. The advantage of ball milling is that it is fully scalable from a few grams to kilogram quantities in a matter of hours.

Additionally, since the entire process is effectively a solid-state process, the materials are inherently unfunctionalized,

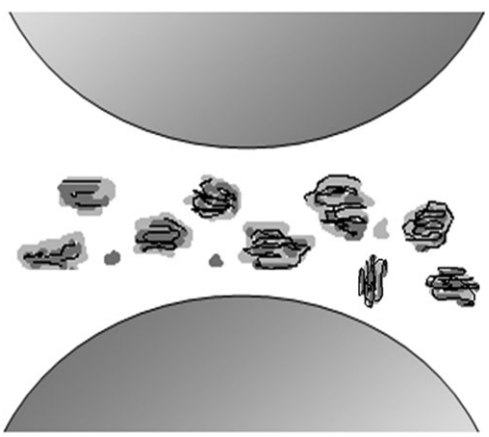

Fig. 9 A schematic of the ball milling process, elemental powders or intermetallic compounds are loaded into a milling vial with some ball bearings. The vial is then loaded into a high energy ball mill. The constant agitation of the ball mill causes the powders to be subjected to a series of impact collisions between the powder and ball bearings.[99,100]

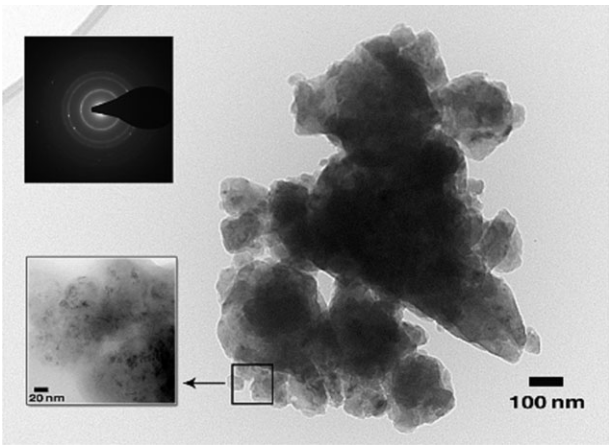

Fig. 10 TEM image of nanostructured silicon prepared *via* ball milling. Large aggregates of crystalline Si nanoparticles are formed. Higher resolution TEM (bottom left inset) shows that the aggregates are made up of small crystallites on the order of 15 nm.[20] An electron diffraction pattern (top left inset) shows crystallinity of the nanoparticles. [Reproduced with permission from ref. 20. Copyright 2009 Wiley-VCH Verlag GmbH & Co. KGaA.]

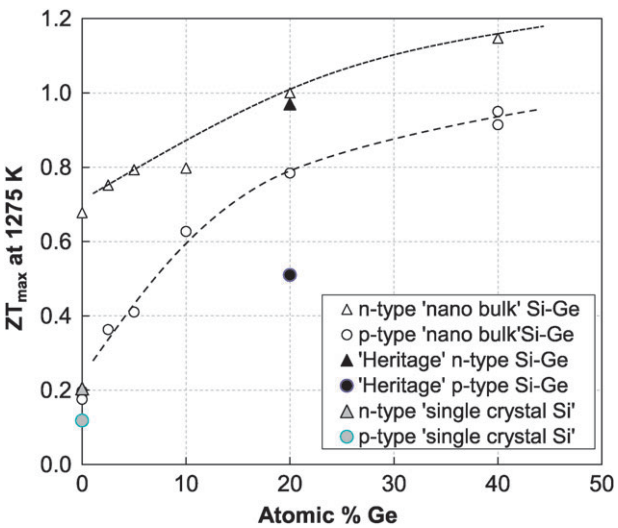

Fig. 11 ZT_{max} at 1275 K for n- and p-type SiGe with increasing Ge content.[115] [Adapted with permission from ref. 115. Copyright 2009 Materials Research Society.]

if handled properly under inert conditions. Once the powders are synthesized, they can be hot-pressed into dense pellets. The consolidated pellets sinter well due to the lack of materials interfering with the grain boundaries and can approach 95 to 100% of the theoretical density.

In addition to pure Si, this technique has recently yielded several promising results in particular with Bi_2Te_3[105] and $Si_{1-x}Ge_x$[104,106] with some of the highest reported ZTs for bulk material systems. The common thread in all of the materials with high ZT produced *via* the ball milling technique is that they are extremely dense (up to 100% of theoretical density) materials that exhibit substantial reductions in the lattice thermal conductivity. The reduced lattice thermal conductivity

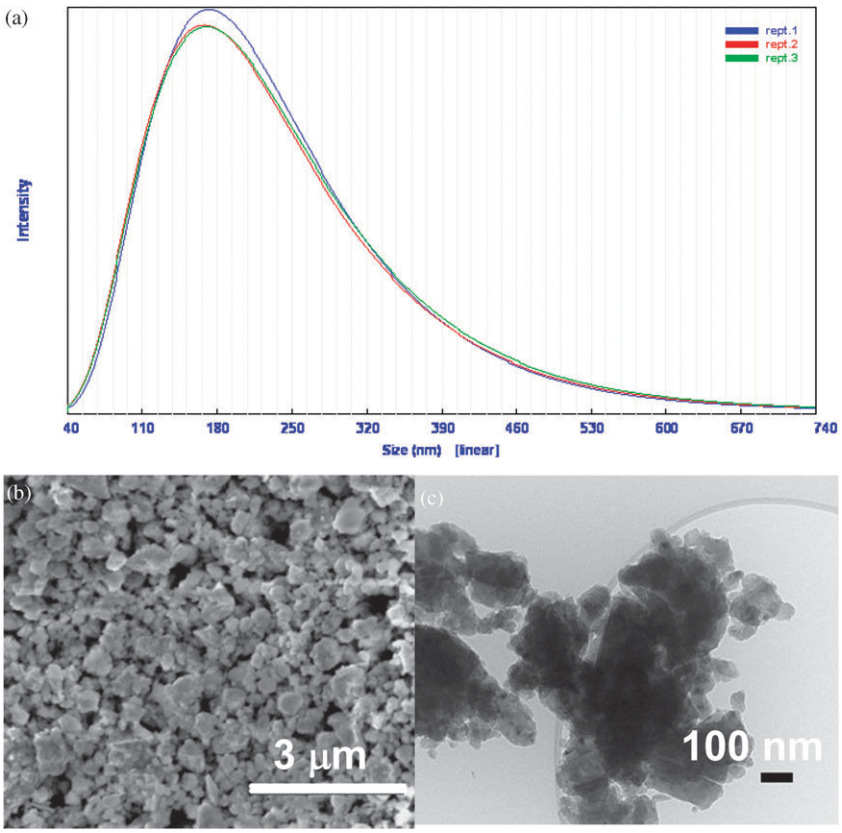

Fig. 12 Particle size characterization of the product produced by ball milling technique: (a) Dynamic light scattering shows a large distribution of nanoparticles from 30 nm to micron sized aggregates. (b) An SEM image confirms the distribution of the particle sizes. (c) A TEM image shows that the aggregates are made up of smaller nanoparticles.

coupled with only a slightly reduced mobility yields ZT increases up to 250%.

3.4.b Disadvantages of the ball milling technique. Although there have been promising results using ball milling, there are also several disadvantages. The distribution of the nanoparticles and the crystallite domains can be difficult to control. Fig. 12a shows a dynamic light scattering spectrum of a sample that was produced *via* the ball milling process. The particle size ranges from 20 nm to 200 nm. This is confirmed by SEM (Fig. 12b). High resolution TEM (Fig. 12c) shows that the aggregates are actually made up of smaller particles and crystallites on the order of 15 nm.

Extended milling in order to generate smaller nanoscale domains can cause contamination from the milling media and wear on the mill. It can also cause defects, which can affect the electronic properties.[20] Additionally, it has also been shown that ball milling can induce strain into a crystal lattice thereby degrading the electrical properties.[116]

4. Consolidation and densification of thermoelectric materials

There is a significant amount of research being conducted on the synthesis of nanostructured materials, however, in order for a material to be practical for an actual thermoelectric device, it must be consolidated into a densified bulk pellet. Fig. 13 shows a picture of a large 70 mm puck (~99% of theoretical density) that can then be machined into the legs needed for a device.

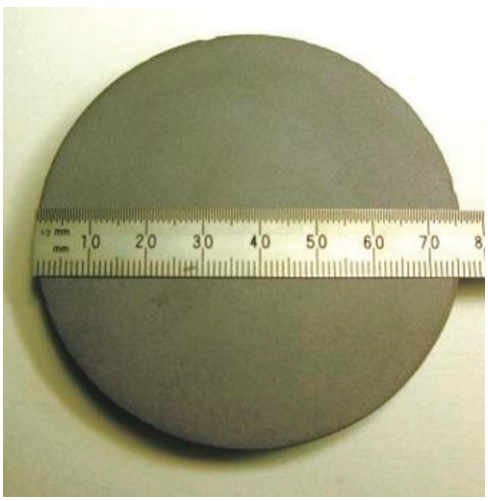

Fig. 13 Large puck to be used for machining thermoelectric couples.

Low density materials typically have poor mechanical properties and are difficult to work with. Numerous studies on porosity indicate that electrical properties can degrade by orders of magnitude when a sample is not at full theoretical density.[117–119] This is due to additional charge scattering and disruption in the mean-free path of the electron as it travels

from one grain to another. Porosity has also been determined to affect thermal conductivity results.[83] Total thermal conductivity, λ, is the product of the thermal diffusivity α, heat capacity C_p, and density ρ (eqn (4)).

$$\lambda = \alpha\rho C_p \quad (4)$$

Since one of the parameters of the thermal conductivity is density, a material with low density will inherently have a low thermal conductivity. Additionally, the pores can act as phonon scattering sites, thereby reducing the lattice thermal conductivity. Theoretically, the ideal nanostructured inclusion for reducing thermal conductivity is a nanoscale void, however, in order for a void to be an effective phonon scatterer it needs to be on the order of a few nanometres.[120] Therefore, when examining the impact of nanostructuring on the thermoelectric properties, it is critical that materials that are being evaluated have similar high densities.

There are three leading methods that are commonly employed in the densification of nanostructured materials: cold-pressing then sintering, hot uniaxial compaction (hot-pressing), and spark plasma sintering (SPS). A relatively new technique that can be used to sinter "softer" materials is known as combustion driven compaction.

4.1.a Cold-pressing. In the cold-pressing then sintering technique, the materials are loaded into a die (usually stainless steel) and hydrostatic pressures of about 5 tons are applied, typically using a Carver press. The pellet is then extracted and heated to about 70% of its theoretical melting point in order to sinter the nanopowder. This process works well for lower melting, "soft" systems such as Bi_2Te_3 and PbTe,[121] where the low bulk modulus yields well to the high pressure compaction. If done correctly, samples of up to 90 percent of the theoretical density can be achieved.[122]

4.1.b Hot-pressing. In the hot-pressing technique, the material is first loaded into a graphite die and then into the press.[123] Pressure is applied in one direction, while the sample is heated throughout to about 70% of its theoretical melting point using graphite or ceramic heating elements.[124,125] The density of the compact typically reaches 95 to 100% of the theoretical density.[126,127] This compaction technique can be used for a variety of materials.

4.1.c Spark plasma sintering. A related method to hot-pressing is spark plasma sintering (SPS). There are varying names for the process, however, the basic technique differs from hot-pressing in that a *pulsed direct current* is conducted through graphite dies under hydrostatic uniaxial pressure. As a result, high temperatures are achieved relatively quickly (minutes as opposed to hours in most hot-presses).[128,129] The extracted pellets can have densities that approach 95–100% of the theoretical density. It is thought that since SPS requires relatively short sintering times, this can prevent grain coarsening of the nanoparticles, effectively keeping them small.[90] However, this remains to be seen experimentally.

4.1.d Combustion driven compaction. A relatively new technique of compacting materials using extremely high pressures

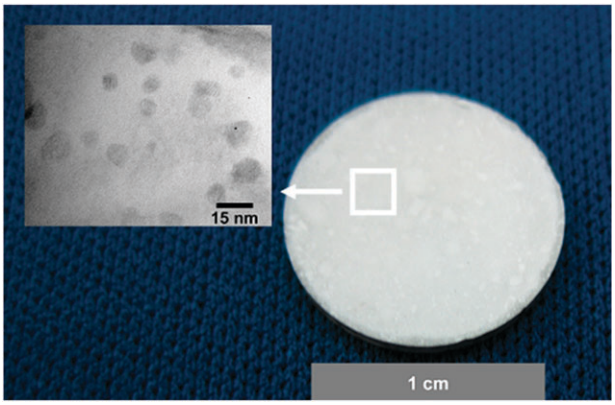

Fig. 14 A fully dense nanostructured Si disk, the inset is a TEM image of an ion milled pellet showing that nanostructured domains remain after high temperature processing.[20] [Adapted with permission from ref. 20. Copyright 2009 Wiley-VCH Verlag GmbH & Co. KGaA.]

is *via* combustion driven compaction. In this process, a pressurized gas based mixture undergoes a controlled combustion reaction; the energy of the force of the reaction is used to drive upper and lower pistons to generate extreme pressures of up to 1000 metric tons.[130] Unlike hot-pressing, which provides extensive sintering at high temperatures and Spark Plasma Sintering, that relies on very large currents to "fuse" the particle interfaces, this technique provides a different path to densification, with no thermal or electrical energy involved. This high pressure compaction technique allows for materials to be compressed to very high densities without the need for post-sintering. The potential advantage of using this technique is that it could consolidate low bulk modulus nanostructured materials such as Bi_2Te_3 or PbTe to very high densities while maintaining their nanostructures.

Although it is critical to compact samples into fully dense bulk materials, it is also critical to prevent grain growth. The key is optimizing temperature and pressure so that the nanoparticles consolidate, but not coalesce into large grains. This method has been successfully demonstrated in several materials.[20,42,103–107] The TEM images demonstrate that although there has been some grain growth, the nanostructured inclusions (Fig. 14) remain along with nanostructured grain boundaries.

5. Thermal stability

Possibly the most critical test of nanostructured bulk thermoelectric materials is their long-term thermal stability. Thermal stability is a key aspect of a nanostructured thermoelectric device, since for practical applications, thermoelectric devices must operate for extended periods of time, often more than 10 to 15 years. There is no gain in synthesizing nanostructured bulk materials if the nanoscale features coalesce back into large grain bulk materials or segregate into macroscale composites. This is a significant limitation that is commonly seen in low- to mid-temperature range compounds such as Bi_2Te_3, $CoSb_3$ and PbTe. For example, Tritt *et al.* also reported on an increased thermal conductivity likely due to grain growth as a result of thermal annealing.[65] Similar

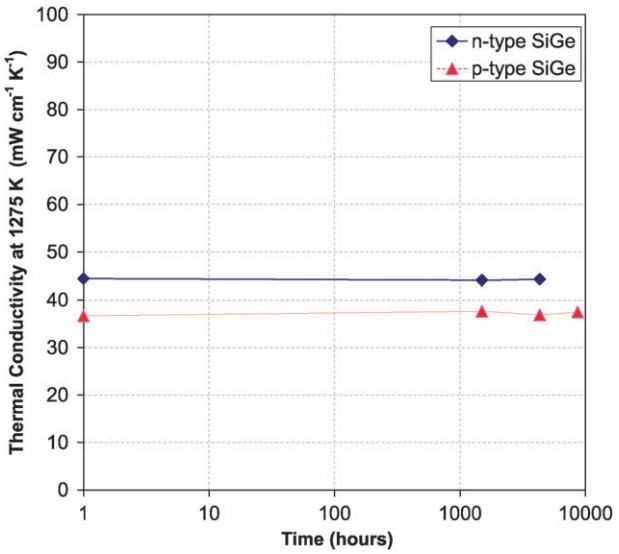

Fig. 15 Thermal stability of n- and p-type nanostructured SiGe over a period of 1 year at 1275 K.[19] Note that there is essentially no change in the thermal conductivity.

problems have also been reported for PbTe based materials.[131] Scheele *et al.* reported a change in the electrical properties of Bi_2Te_3 as a result of post-sintering.[90] This is likely due to grain growth of the nanoparticles reducing the high surface energy.

However, it is possible to have thermally stable nanostructured materials. ''Lifetime'' thermal stability tests at the Jet Propulsion Laboratory on n-type and p-type $Si_{0.80}Ge_{0.20}$ did not show changes in the thermal conductivity values during extended testing for 9000 hours (1 year) at 1275 K under vacuum (Fig. 15).[19] Additionally, 3 month lifetime thermal stability measurements have been done on the LAST compounds by Kanatzidis and co-workers and they showed relatively little change in thermoelectric properties and that the nanostructured inclusions remain. However, the tests were conducted at a relatively low temperature (675 K).[91]

Conclusions

An overview of the multiple synthetic techniques and a guideline as to what is needed for practical thermoelectric applications has been presented. For practical thermoelectric applications the synthetic technique should be: (1) scalable and relatively low cost, with tuneable electrical properties, (2) the nanoscale materials must be able to form dense compacts for machining/device integration, (3) the nanostructured material should demonstrate an enhanced ZT over the bulk material and finally (4) the compacted nanoscale features should be thermally stable for extended periods of time. While several techniques have produced promising ZTs, higher thermoelectric conversion efficiencies are still needed in order to be applicable for large scale applications such as waste heat recovery. With proper optimization of these techniques and elimination of the various problems, nanostructuring could create a promising class of materials for high thermoelectric figure of merit devices.

Acknowledgements

The authors thank Dr Thierry Caillat for his helpful discussions. Support from the National Science Foundation DMR 0805352 (RBK), an IGERT fellowship DGE-0114443 and DGE-0654431 (SKB), a NASA GSRP fellowship NNX09AM26H (SKB), and a JPL/Caltech subcontract 1308818 (RBK) are gratefully acknowledged. Part of this work was performed at the Jet Propulsion Laboratory, California Institute of Technology under contract with the National Aeronautics and Space Administration.

Notes and references

1 C. B. Vining, *Nat. Mater.*, 2009, **8**, 83–85.
2 *CRC Handbook of Thermoelectrics*, ed. D. M. Rowe, CRC, Boca Raton, 1995, 1-1.
3 K. Matsubara, *Proc. Int. Conf. Thermoelectr.*, 2002, **1**, 418.
4 T. Hendricks and W. Choate, U.S. Department of Energy, Industrial Technologies Program, 2008, 1.
5 H. J. Goldsmid, *Electronic Refrigeration*, Pion Ltd., London, 1986.
6 J. Kern, S. Freedman, D. Klett, E. Afify, R. Arndt, W. Stine, A. Armor, C. Jotshi, D. Yogi Goswami, R. Pagano, J. Tulenko, T. Shannon, D. Berg, C. Bliem, G. Mines, K. Reinhardt, M. Ramalingam, J.-P. Fleurial, W. Jackson and A. Lezuo, in *The CRC Handbook of Mechanical Engineering*, 2nd edn, CRC Press, Boca Raton, 2009.
7 T. J. Seebeck, *Abh. Dtsch. Akad. Wiss. Berlin, Kl. Math., Phys. Tech.*, 1825, **1822–1823**, 265.
8 J. C. Peltier, *Ann. Chim. Phys.*, 1834, **56**, 371.
9 C. Wood, *Rep. Prog. Phys.*, 1988, **51**, 459.
10 D. Rowe and C. Bhandari, in *CRC Handbook of Thermoelectrics*, CRC Press, Boca Raton, 1995, 5-1.
11 G. J. Snyder and E. S. Toberer, *Nat. Mater.*, 2008, **7**, 105–114.
12 H. J. Goldsmid and A. W. Penn, *Phys. Lett. A*, 1968, **27**, 523–524.
13 N. K. Abrikosov, K. A. Dyuldina and T. A. Danilyan, *Zh. Neorg. Khim.*, 1958, **3**, 1632.
14 J. P. Dismukes, L. Ekstrom, E. F. Steigmeier, I. Kudman and D. S. Beers, *J. Appl. Phys.*, 1964, **35**, 2899–2907.
15 L. E. Shelimova, P. P. Konstantinov, O. G. Karpinsky, E. S. Avilov, M. A. Kretova and J. P. Fleurial, *Proc. Int. Conf. Thermoelectr.*, 1999, **1**, 536.
16 D. M. Rowe, V. S. Shukla and N. Savvides, *Nature*, 1981, **290**, 765–766.
17 N. Scoville, C. Bajgar, J. Rolfe, J. P. Fleurial and J. Vandersande, *Nanostruct. Mater.*, 1995, **5**, 207–223.
18 J. Vandersande, J. McCormack, A. Zoltan and J. Farmer, *Proc. Intersoc. Energy Convers. Eng. Conf.*, 1990, **2**, 392.
19 T. Caillat, Private Communication, 2010.
20 S. K. Bux, R. G. Blair, P. K. Gogna, H. Lee, G. Chen, M. S. Dresselhaus, R. B. Kaner and J.-P. Fleurial, *Adv. Funct. Mater.*, 2009, **19**, 2445–2452.
21 G. Slack, in *CRC Handbook of Thermoelectrics*, CRC Press, Boca Raton, 1995, 34-1.
22 T. Caillat, J. P. Fleurial and A. Borshchevsky, *Proc. Int. Conf. Thermoelectr.*, 1996, **1**, 100.
23 G. S. Nolas, D. T. Morelli and T. M. Tritt, *Annu. Rev. Mater. Sci.*, 1999, **29**, 89–116.
24 E. S. Toberer, A. F. May and G. J. Snyder, *Chem. Mater.*, 2010, **22**, 624–634.
25 H. Kleinke, *Chem. Mater.*, 2009, **22**, 604–611.
26 P. Rogl, *CRC Thermoelectrics Handbook*, CRC Press, Boca Raton, 2006, 32-1.
27 L. D. Hicks and M. S. Dresselhaus, *Phys. Rev. B: Condens. Matter*, 1993, **47**, 12727.
28 R. Venkatasubramanian, E. Siivola, T. Colpitts and B. O'Quinn, *Nature*, 2001, **413**, 597–602.
29 T. C. Harman, P. J. Taylor, M. P. Walsh and B. E. LaForge, *Science*, 2002, **297**, 2229–2232.
30 A. I. Boukai, Y. Bunimovich, J. Tahir-Kheli, J. K. Yu, W. A. Goddard and J. R. Heath, *Nature*, 2008, **451**, 168–171.

31 A. I. Hochbaum, R. Chen, R. D. Delgado, W. Liang, E. C. Garnett, M. Najarian, A. Majumdar and P. Yang, *Nature*, 2008, **451**, 163–167.
32 D. Vashaee and A. Shakouri, *Phys. Rev. Lett.*, 2004, **92**, 106103.
33 W. Kim, S. L. Singer, A. Majumdar, D. Vashaee, Z. Bian, A. Shakouri, G. Zeng, J. E. Bowers, J. M. O. Zide and A. C. Gossard, *Appl. Phys. Lett.*, 2006, **88**, 242107–242103.
34 S. M. Lee, D. G. Cahill and R. Venkatasubramanian, *Appl. Phys. Lett.*, 1997, **70**, 2957–2959.
35 Y. Bao, W. L. Liu, M. Shamsa, K. Alim, A. A. Balandin and J. L. Liu, *J. Electrochem. Soc.*, 2005, **152**, G432–G435.
36 D. Vashaee and A. Shakouri, *J. Appl. Phys.*, 2007, **101**, 053719–053715.
37 A. Shakouri and M. Zebarjadi, in *Thermal Nanosystems and Nanomaterials*, Springer-Verlag, Berlin, 2009, pp. 225–299.
38 G. Chen, M. S. Dresselhaus, G. Dresselhaus, J. P. Fleurial and T. Caillat, *Int. Mater. Rev.*, 2003, **48**, 45.
39 H. Bottner, G. Chen and R. Venkatasubramanian, *MRS Bull.*, 2006, **31**, 211.
40 R. Venkatasubramanian, *CRC Thermoelectrics Handbook*, CRC Press, Boca Raton, 2006, 49-1.
41 Y. K. Koh, C. J. Vineis, S. D. Calawa, M. P. Walsh and D. G. Cahill, *Appl. Phys. Lett.*, 2009, **94**, 153101.
42 M. S. Dresselhaus, G. Chen, M. Y. Tang, R. G. Yang, H. Lee, D. Z. Wang, Z. F. Ren, J. P. Fleurial and P. Gogna, *Adv. Mater.*, 2007, **19**, 1043–1053.
43 D. L. Medlin and G. J. Snyder, *Curr. Opin. Colloid Interface Sci.*, 2009, **14**, 226–235.
44 S. Scherrer and H. Scherrer, *CRC Handbook of Thermoelectrics*, CRC Press, Boca Raton, 1995, 19-1.
45 V. Fano, *CRC Handbook of Thermoelectrics*, CRC Press, Boca Raton, 1995, 21-1.
46 C. Uher, *CRC Thermoelectrics Handbook*, CRC Press, Boca Raton, 2006, 34-1.
47 C. Vining, *CRC Handbook of Thermoelectrics*, CRC Press, Boca Raton, 1995, 23-1.
48 G. D. Mahan, in *Solid State Physics*, ed. H. Ehrenreich and F. Spaepne, Academic Press, New York, 1997, p. 81.
49 A. Henry and G. Chen, *J. Comput. Theor. Nanosci.*, 2008, **5**, 141.
50 M. A. Ryan, J. A. Harman, J. P. Fleurial, J. Whitacre, R. M. Williams, G. J. Snyder, D. Daly, C.-K. Huang, T. Caillat and A. Borshchevsky, *Proc.–Electrochem.Soc.*, 2000, **22**, 229.
51 E. J. Menke, M. A. Brown, Q. Li, J. C. Hemminger and R. M. Penner, *Langmuir*, 2006, **22**, 10564–10574.
52 D. J. Riley, *Curr. Opin. Colloid Interface Sci.*, 2002, **7**, 186–192.
53 M. T. Swihart, *Curr. Opin. Colloid Interface Sci.*, 2003, **8**, 127–133.
54 A. Reau, B. Guizard, C. Mengeot, L. Boulanger and F. Tenegal, *Mater. Sci. Forum*, 2007, **1**, 534.
55 K. T. Wojciechowski and J. Morgiel, *Proc. Int. Conf. Thermoelectr.*, 2003, **1**, 97.
56 A. Bapat, *et al.*, *Plasma Phys. Controlled Fusion*, 2004, **46**, B97.
57 X. Ji, B. Zhang, T. M. Tritt, J. W. Kolis and A. Kumbhar, *J. Electron. Mater.*, 2007, **36**, 721.
58 Y. H. Zhang, T. J. Zhu, J. P. Tu and X. B. Zhao, *Mater. Chem. Phys.*, 2007, **103**, 484–488.
59 J. L. Mi, T. J. Zhu, X. B. Zhao and J. Ma, *J. Appl. Phys.*, 2007, **101**, 054314.
60 X. B. Zhao, X. H. Ji, Y. H. Zhang and B. H. Lu, *J. Alloys Compd.*, 2004, **368**, 349–352.
61 X. Zhao, *CRC Thermoelectrics Handbook*, CRC Press, Boca Raton, 2006, 25-1.
62 S. H. Yu, J. Yang, Y. S. Wu, Z. H. Han, J. Lu, Y. Xie and Y. T. Qian, *J. Mater. Chem.*, 1998, **8**, 1949.
63 M. Salavati-Niasari, M. Bazarganipour and F. Davar, *J. Alloys Compd*, 2010, **489**, 530–534.
64 M. Toprak and M. Muhammed, *CRC Thermoelectrics Handbook*, CRC Press, Boca Raton, 2006, 41-1.
65 X. Ji, P. Alboni, Z. Su, N. Gothard, B. Zhang, T. M. Tritt and J. W. Kolis, *Phys. Status Solidi RRL*, 2007, **1**, 229–231.
66 J. Q. Li, X. W. Feng, W. A. Sun, W. Q. Ao, F. S. Liu and Y. Du, *Mater. Chem. Phys.*, 2008, **112**, 57–62.
67 Y. Deng, X.-s. Zhou, G.-d. Wei, J. Liu, C.-W. Nan and S.-j. Zhao, *J. Phys. Chem. Solids*, 2002, **63**, 2119–2121.
68 X. Ji, J. He, Z. Su, N. Gothard and T. M. Tritt, *J. Appl. Phys.*, 2008, **104**, 034907–034906.
69 T. Caillat, *J. Phys. Chem. Solids*, 1996, **57**, 1351–1358.
70 M. R. Dirmyer, J. Martin, G. S. Nolas, S. Ayusman and J. V. Badding, *Small*, 2009, **5**, 933–937.
71 G. Zhang, Q. Yu and X. Li, *Dalton Trans.*, 2010, **39**, 993–1004.
72 Y. Zhao, J. S. Dyck, B. M. Hernandez and C. Burda, *J. Am. Chem. Soc.*, 2010, **132**, 4982–4983.
73 Y. Zhao and C. Burda, *ACS Appl. Mater. Interfaces*, 2009, **1**, 1259–1263.
74 Z. Sun, S. Liufu, Q. Yao and L. Chen, *Mater. Chem. Phys.*, 2010, **121**, 138–141.
75 L. Yang, H. H. Hng, H. Cheng, T. Sun and J. Ma, *Mater. Lett.*, 2008, **62**, 2483–2485.
76 C. Stiewe, L. Bertini, M. Toprak, M. Christensen, D. Platzek, S. Williams, C. Gatti, E. Muller, B. B. Iversen, M. Muhammed and M. Rowe, *J. Appl. Phys.*, 2005, **97**, 044317.
77 M. Toprak, Y. Zhang, M. Muhammed, A. A. Zakhidov, R. H. Baughman and I. Khayrullin, *Proc. Int. Conf. Thermoelectr.*, 1999, **1**, 382.
78 L. Yang, H. H. Hng, D. Li, Q. Y. Yan, J. Ma, T. J. Zhu, X. B. Zhao and H. Huang, *J. Appl. Phys.*, 2009, **106**, 013705.
79 Y. Y. Wang, K. F. Cai and X. Yao, *J. Solid State Chem.*, 2009, **182**, 3383–3386.
80 B. Wan, C. Hu, B. Feng, Y. Xi and X. He, *Mater. Sci. Eng., B*, 2009, **163**, 57–61.
81 W. Zhang, L. Zhang, Y. Cheng, Z. Hui, X. Zhang, Y. Xie and Y. Qian, *Mater. Res. Bull.*, 2000, **35**, 2009–2015.
82 T. J. Zhu, Y. Q. Cao, Q. Zhang and X. B. Zhao, *J. Electron. Mater.*, 2009, **39**, 1990.
83 J. Martin, G. S. Nolas, W. Zhang and L. Chen, *Appl. Phys. Lett.*, 2007, **90**, 222112.
84 J. Martin, L. Wang, L. Chen and G. S. Nolas, *Phys. Rev. B: Condens. Matter*, 2009, **79**, 115311.
85 D. Neiner, H. W. Chiu and S. M. Kauzlarich, *J. Am. Chem. Soc.*, 2006, **128**, 11016–11017.
86 A. P. Alivisatos, *Science*, 1996, **271**, 933–937.
87 W. Lu, J. Fang, K. L. Stokes and J. Lin, *J. Am. Chem. Soc.*, 2004, **126**, 11798–11799.
88 X. G. Peng, L. Manna, W. D. Yang, J. Wickham, E. Scher, A. Kadavanich and A. P. Alivisatos, *Nature*, 2000, **404**, 59–61.
89 T. Durst, H. J. Goldsmid and L. B. Harris, *Sol. Energy Mater.*, 1981, **5**, 181–186.
90 M. Scheele, N. Oeschler, K. Meier, A. Koronowski, C. Klinke and H. Weller, *Adv. Funct. Mater*, 2009, **19**, 3476.
91 M. G. Kanatzidis, *Chem. Mater.*, 2009, **22**, 648–659.
92 K. F. Hsu, S. Loo, F. Guo, W. Chen, J. S. Dyck, C. Uher, T. Hogan, E. K. Polychroniadis and M. G. Kanatzidis, *Science*, 2004, **303**, 818–821.
93 T. Ikeda, L. A. Collins, V. A. Ravi, F. S. Gascoin, S. M. Haile and G. J. Snyder, *Chem. Mater.*, 2007, **19**, 763–767.
94 B. A. Cook, M. J. Kramer, J. L. Harringa, M.-K. Han, D.-Y. Chung and M. G. Kanatzidis, *Adv. Funct. Mater.*, 2009, **19**, 1254–1259.
95 J. R. Sootsman, D. Y. Chung and M. G. Kanatzidis, *Angew. Chem., Int. Ed.*, 2009, **48**, 8616–8639.
96 Y. Gelbstein, B. Dado, O. Ben-Yehuda, Y. Sadia, Z. Dashevsky and M. P. Dariel, *Chem. Mater.*, 2009, **22**, 1054–1058.
97 T. J. Zhu, *et al.*, *J. Phys. D: Appl. Phys.*, 2007, **40**, 3537.
98 Y. Q. Cao, X. B. Zhao, T. J. Zhu, X. B. Zhang and J. P. Tu, *Appl. Phys. Lett.*, 2008, **92**, 143106.
99 C. Suryanarayana, *Prog. Mater. Sci.*, 2001, **46**, 1–184.
100 J. Harringa, B. Cook and S. Han, *CRC Handbook of Thermoelectrics*, CRC Press, Boca Raton, 1995, 12-1.
101 T. Ikeda, E. S. Toberer, V. A. Ravi, S. M. Haile and G. J. Snyder, *Proc. Int. Conf. Thermoelectr. Energy Convers.*, 2007, 1.
102 T. Ikeda, Private Communication, 2010.
103 M. S. Dresselhaus, C. Gang, R. Zhifeng, J. P. Fleurial, P. Gogna, M. Y. Tang, D. Vashaee, L. Hohyun, W. Xiaowei, G. Joshi, Z. Gaohua, W. Dezhi, R. Blair, S. Bux and R. Kaner, in *Thermoelectric Power Generation*, Materials Research Society, 2008, pp. 29–41.
104 G. Joshi, H. Lee, Y. Lan, X. Wang, G. Zhu, D. Wang, R. W. Gould, D. C. Cuff, M. Y. Tang, M. S. Dresselhaus, G. Chen and Z. Ren, *Nano Lett.*, 2008, **8**, 4670–4674.

105 B. Poudel, Q. Hao, Y. Ma, Y. Lan, A. Minnich, B. Yu, X. Yan, D. Wang, A. Muto, D. Vashaee, X. Chen, J. Liu, M. S. Dresselhaus, G. Chen and Z. Ren, *Science*, 2008, **320**, 634–638.
106 X. W. Wang, H. Lee, Y. C. Lan, G. H. Zhu, G. Joshi, D. Z. Wang, J. Yang, A. J. Muto, M. Y. Tang, J. Klatsky, S. Song, M. S. Dresselhaus, G. Chen and Z. F. Ren, *Appl. Phys. Lett.*, 2008, **93**, 3.
107 G. H. Zhu, H. Lee, Y. C. Lan, X. W. Wang, G. Joshi, D. Z. Wang, J. Yang, D. Vashaee, H. Guilbert, A. Pillitteri, M. S. Dresselhaus, G. Chen and Z. F. Ren, *Phys. Rev. Lett.*, 2009, **102**, 196803.
108 A. Minnich, M. S. Dresselhaus, Z. F. Ren and G. Chen, *Energy Environ. Sci.*, 2009, **2**, 466–479.
109 Y. Lan, A. J. Minnich, G. Chen and Z. Ren, *Adv. Funct. Mater.*, 2010, **20**, 357–376.
110 J. Benjamin, *Metall. Mater. Trans. B*, 1970, **1**, 2943–2951.
111 J. Schilz, M. Riffel, K. Pixius and H. J. Meyer, *Powder Technol.*, 1999, **105**, 149–154.
112 T. Caillat, J. P. Fleurial and A. Borshchevsky, *Proc. Int. Conf. Thermoelectr.*, 1992, **1**, 240.
113 B. A. Cook, B. J. Beaudry, J. L. Harringa and W. J. Barnett, *Proc. Intersoc. Energy Convers. Eng. Conf.*, 1989, **2**, 693.
114 S. K. Bux, R. G. Blair, P. K. Gogna, H. Lee, G. Chen, M. S. Dresselhaus, R. B. Kaner and J. P. Fleurial, *Adv. Funct. Mater.*, 2009, **19**, 2445–2452.
115 S. Bux, J. P. Fleurial, R. Blair, P. Gogna, T. Caillat and R. Kaner, in *Materials Research Society Spring 2009 Meeting*, ed. J. Yang, G. S. Nolas, K. Koumoto and Y. Grin, Materials Research Society, San Francisco, CA, 2009, pp. 1166-N1102-1104.
116 J. P. Heremans, C. M. Thrush and D. T. Morelli, *Phys. Rev. B: Condens. Matter*, 2004, **70**, 115334.
117 I. Sumirat, Y. Ando and S. Shimamura, *J. Porous Mater.*, 2006, **13**, 439.
118 A. J. Crocker and L. M. Rogers, *Br. J. Appl. Phys.*, 1967, **18**, 563.
119 F. Euler, *J. Appl. Phys.*, 1957, **28**, 1342–1345.
120 H. Goldsmid, *Materials*, 2009, **2**, 903–910.
121 D. R. Thornburg, F. Emley and D. H. Lane, *Mod. Develop. Powder Met., Proc. Int. Powder Met. Conf.*, 1966, **3**, 138.
122 S.-C. Ur, I.-H. Kim and P. Nash, *J. Mater. Sci.*, 2007, **42**, 2143–2149.
123 F. B. Swinkels, D. S. Wilkinson, E. Arzt and M. F. Ashby, *Acta Metall.*, 1983, **31**, 1829–1840.
124 S. R. Gupta and H. Singh, *Phys. Status Solidi A*, 1971, **8**, 267–270.
125 A. Nancy Scoville, *CRC Handbook of Thermoelectrics*, CRC Press, Boca Raton, 1995, 10-1.
126 P. R. Sahm, *Mater. Res. Bull.*, 1967, **2**, 85–89.
127 N. Savvides and H. J. Goldsmid, *J. Mater. Sci.*, 1980, **15**, 594–600.
128 M. Omori, *Mater. Sci. Eng., A*, 2000, **287**, 183–188.
129 Z. Munir, U. Anselmi-Tamburini and M. Ohyanagi, *J. Mater. Sci.*, 2006, **41**, 763–777.
130 K. Nagarathnam, A. Renner, D. Trostle, D. Kruczynaski and D. Massey, Development of 1000-Ton Combustion Driven Compaction Press for Materials Development and Processing, http://www.utroninc.com/PowderMet2007-PaperPress.pdf, Accessed May 17, 2010.
131 B. Paul and P. Banerji, *Nanosci. Nanotechnol. Lett.*, 2009, **1**, 208–212.

